

42p

(NASA TML 21144)

N65-88976

~~X64 10509~~

CODE-2A

THE IDEALIZED STEADY-STATE INTERACTION OF THE
GEOMAGNETIC FIELD AND THE SOLAR CORPUSCULAR RADIATION

Ronald Blum* 1963 42p

refs Submitted
for publication

6021281 NASA
Goddard Institute for Space Studies,
National Aeronautics & Space Administration
New York 27, N.Y.

Available to NASA Offices and
NASA Centers Only.

*National Academy of Sciences -- National Research
Council, Post-doctoral Research Associate with NASA.

INTRODUCTION

Experiment and theory agree [Blum, 1963a] that the solar corona is continually expanding throughout the solar system in the form of a tenuous, fully-ionized plasma, the solar corpuscular radiation (SCR). This plasma interacts with the geomagnetic field (GMF) to confine it within a finite cavity, the magnetosphere. This cavity is approximately $10R_e$ (earth radius, $R_e = 6400$ km) in its smallest dimension, and is separated from the SCR by an interface, the magnetopause, which is less than 200 km in thickness. It also appears likely -- although this has not been directly observed as yet -- that the flow of SCR around the magnetosphere is modified by the presence of a stationary collisionless shock on the sunward (upstream) side.

In attempting to find an approximate solution to the magnetosphere geometry we shall employ the idealized model of Beard [1960], which assumes a magnetic dipole of moment M (Fig. 1) immersed in a field-free plasma, perpendicular to the stream direction. With the exception of the dipole singularity at the origin of coordinates, the magnetic field potentials must satisfy Laplace's equation within the (assumed) plasma-free magnetosphere. On the surface of the magnetosphere (the magnetopause is neglected) two boundary conditions are to be satisfied:

(1) the magnetic field is completely confined within the cavity and has no component normal to the surface; (2) the magnetic pressure inside the surface equals the kinetic pressure due to the impact of SCR incident upon the surface.

In this paper we shall develop a method which may be used to obtain approximate solutions to this problem. The method consists in finding two families of surfaces, each family satisfying one of the two boundary conditions identically on the noon meridian contour (NMC) of the magnetosphere (Fig. 1, line ANB). The intersection of the two families is the desired solution. The first, or F-family, involves the vector potential; the second, or G-family, involves the scalar potential of the field in the magnetosphere. The potentials are expanded in a series of solutions of Laplace's equation appropriate to the geometry and the source field. The series coefficients are determined by requiring that the F- and G-surface intersect at a number of arbitrarily selected points on contour ANB (Fig. 1).

The basic assumption of the method is that if the F- and G-surfaces approximately coincide over a region whose dimensions are at least of the order of the magnetosphere dimensions, then they approximately coincide with the actual free boundary in that region. Furthermore, in determining the potentials we have also found

an approximate solution for the fields. We then calculate the shape of the entire magnetosphere numerically and verify the accuracy with which the approximation satisfies the boundary conditions.

This method has been compared, in two dimensions, with the exact solutions of Hurley [1961a,b] and has been shown to give good approximations (within a few per cent) of Hurley's results, without the necessity of any further assumptions [Blum, 1963b].

BOUNDARY CONDITIONS

The confinement condition may be expressed as a Neumann condition on the magnetic scalar potential:

$$\partial\Omega/\partial n = 0 \quad , \quad (1)$$

where n is in the direction normal to the surface of the magnetosphere. The magnetic field, \underline{H} , may be derived from either a scalar or a vector potential:

$$\underline{H} = - \text{grad } \Omega = \text{curl } \underline{A} \quad . \quad (2)$$

Dungey [1958, Chap. 8] has shown that in an ideal, steady-state case of SCR impinging upon a one-dimensional, dipole-like field we expect the plasma particles to be specularly reflected from the magnetopause. Thus the pressure condition on the boundary is

$$H^2/8\pi = 2n_0 m V^2 \cos^2 \chi \quad (3)$$

where n_0 is the density of the SCR, V is its velocity, m the mass of a hydrogen atom, and χ the angle the incident plasma stream makes with the normal to the surface (Fig. 1). However, considering the great magnetohydrodynamic activity found in the region of the magnetopause it might be more correct to assume diffuse reflection, or even no reflection at all. Therefore, we shall take our second boundary condition to be

$$H^2 = \beta^2 \cos^2 \chi, \quad \beta^2 = kn_0 m V^2 \quad (4)$$

where k is a constant, $1 \leq k \leq 2$. The choice of k will have only a small effect on the dimensions of the magnetosphere, since $H \sim 1/L^3$. In hypersonic flow theory this condition (Eq. (4)) is commonly known as Newton's condition ($k = 1$) and has been shown empirically to hold very closely for gaseous flow around the blunt body behind a detached shock wave [Hayes and Probstein, 1959, Chap. III], so that this condition should remain approximately valid even if there does exist a detached shock wave upstream of the magnetosphere.

This idealized three-dimensional free-boundary problem has thus far not been solved; our goal is to develop an approximation which may ultimately be brought to a high degree of accuracy.

THE METHOD -- NOON MERIDIAN CONTOUR

To describe this problem we shall employ spherical coordinates (r, θ, ϕ) as shown in Fig. 1. Note that the magnetic dipole is taken parallel to the x-axis, which it is customary to show pointing north; in our case, therefore, x points south. The SCR is moving in the negative z-direction. We expect the correct solution to include a neutral point, N, which should be located on the NMC on the dayside of the magnetosphere. For convenience, the term "noon meridian contour" will be understood to include the midnight meridian as well.

The scalar potential, Ω , must satisfy Laplace's equation:

$$\nabla^2 \Omega = \frac{\partial}{\partial r} \left(r^2 \frac{\partial \Omega}{\partial r} \right) + \csc \theta \frac{\partial}{\partial \theta} \left(\sin \theta \frac{\partial \Omega}{\partial \theta} \right) + \csc^2 \theta \frac{\partial^2 \Omega}{\partial \phi^2} = 0, \quad (5)$$

and a corresponding vector potential, \underline{A} , can be derived from the scalar $W(r, \theta, \phi)$:

$$\underline{A} = \underline{\nabla} \times (\underline{r}W) ; \nabla^2 W = 0. \quad (6)$$

If we denote the undisturbed components of the potentials by the subscript $(_0)$ and the components induced by the GMF-SCR interaction by primes ($'$), the geomagnetic dipole potentials are

$$\begin{aligned} \Omega_0 &= (M/r^2) \sin \theta \cos \phi; \\ \underline{A}_0 &= - (M/r^2) (\underline{\theta} \sin \phi + \underline{\phi} \cos \theta \cos \phi), \end{aligned} \quad (7)$$

and

$$\underline{A}_0 = \underline{\nabla} \times (\underline{r}W_0), \quad W_0 = \Omega_0, \quad (8)$$

where $\underline{\theta}$ and $\underline{\phi}$ are unit vectors in the θ and ϕ directions, and \underline{r} is the radius vector.

The induced scalar potential, Ω' , must also satisfy Laplace's equation, and because it cannot be singular within the magnetosphere we select the form

$$\Omega' = \sum_{n=1}^{\infty} \sum_{m=1}^n B_{nm} r^n P_n^m(\cos \theta) \cos m\phi, \quad m \text{ odd}; \quad (9)$$

$P_n^m(\cos \theta)$ is the associated Legendre polynomial. The $\cos m\phi$ dependence is determined by the fact that the problem is symmetric about the xz-plane. We also argue that in the equatorial plane symmetry requires $H = H \underline{\phi}$. The other components of \underline{H} will vanish identically if m is an odd integer; in that case $\cos(m\pi/2) = 0$.

The induced magnetic field may also be derived from the vector potential

$$\begin{aligned} \underline{A}' &= \underline{\nabla} \times (\underline{r} W'); \quad \nabla^2 W' = 0 \\ W' &= \sum_{n=1}^{\infty} \sum_{m=1}^n A_{nm} R^n P_n^m(\cos \theta) \cos m\phi, \quad m \text{ odd} \\ B_{nm} &= -(n+1) A_{nm} \end{aligned} \quad (10)$$

Next we consider fields and potentials on the NMC, where the magnetic field must, by symmetry, lie in the noon meridian plane. By definition it is clear that $\cos^2 \chi = (dx/ds)^2$ (see Fig. 2), and Eq. (4) becomes

$$H = \pm B dx/ds. \quad (11)$$

Upon multiplication by β we find:

$$-d\Omega = Hds = \pm \beta dx, \quad (12)$$

where $d\Omega$ represents the change in Ω along the NMC. Thus, if we construct a contour in space,

$$G(r, \theta) = \begin{cases} -G^- = -\Omega(r, \theta, 0) + \beta r \sin \theta + K^- = 0, & 0 \leq \theta \leq \theta_N; \\ G^+ = \Omega(r, \theta, 0) + \beta r \sin \theta - K^+ = 0, & \theta_N \leq \theta \leq \pi; \end{cases} \quad (13)$$

$$(\Phi = 0)$$

where K^\pm are arbitrary constants, θ_N is the neutral point, and $K^- = 0$ (since $P_n^m(1) = 0$ for $m \geq 1$), we can see that the component of $\underline{H} = -\underline{\nabla}\Omega$ tangential to this contour has the property

$$H_s^2 = \beta^2 \cos^2 \chi. \quad (14)$$

If we could, in some manner, insure that the normal component of \underline{H} on the G-contour would vanish, then $\underline{H} = \underline{H}_s$, and G would represent the NMC. Although G is a uniquely defined function of Ω we cannot be sure that it is the only contour on which Ω would satisfy the boundary conditions. However, for the purpose of this argument we shall assume that it is.

The next step is to find some prescription which will make the normal component of \underline{H} vanish on G. This

is done by requiring that ϕ coincide with some F-surface which is in turn defined to be tangential to \underline{H} .

In order to find a suitable representation for F we note that it must satisfy ($\phi = 0$)

$$\underline{H} \cdot \underline{\nabla} F = (\underline{\nabla} \times \underline{A}) \cdot \underline{\nabla} F = [(2 + r \partial/\partial r) \underline{\nabla} W] \cdot \underline{\nabla} F = 0, \quad (15)$$

and since $W = W_0 + W'$ satisfies Laplace's equation, we may substitute

$$r(2+r\partial/\partial r)(\partial W/\partial r) = -\csc \theta (\partial/\partial \theta)(\sin \theta \partial W/\partial \theta) - \csc^2 \theta \partial^2 W/\partial \phi^2 \quad (16)$$

into Eq. (15). By symmetry, if $F = F(r, \theta, \phi)$, then we have $H_\phi = 0$ on the NMC, so that Eq. (15) reduces to

$$\begin{aligned} r(\partial F/\partial r) \left[\frac{\partial}{\partial \theta} (\sin \theta \partial W/\partial \theta) + \csc \theta \frac{\partial^2 W}{\partial \phi^2} \right] \\ = \sin \theta (\partial F/\partial \theta) \left[\frac{\partial W}{\partial \theta} + r \frac{\partial^2 W}{\partial r \partial \theta} \right]. \end{aligned} \quad (17)$$

for $\phi = 0$. If we set

$$F(r, \theta, \phi) = r \cos \theta \partial W/\partial \theta - C = 0 \quad (18)$$

and substitute into Eq. (17), we find

$$\left(\sin \theta \frac{\partial W}{\partial \theta} + \cos \theta \frac{\partial^2 W}{\partial \phi^2} \right) \left(\frac{\partial W}{\partial \theta} + r \frac{\partial^2 W}{\partial r \partial \theta} \right) = 0 \quad (19)$$

If the representation suggested in Eq. (18) is to satisfy Eq. (15), we shall need to impose another condition

on W ; viz., that the left-hand factor of Eq. (19) be identically zero for all (r, θ) as long as $\bar{\phi} = 0$. We shall term this the "congruence condition." We note that W_0 already satisfies this condition. If we substitute for W' from Eq. (10) the congruence condition on W reduces to

$$\sum_{m=1}^{m \leq n} A_{nm} \left(\sin \theta \frac{d P_n^m(\cos \theta)}{d \theta} - m^2 \cos \theta P_n^m(\cos \theta) \right) = 0$$

$m \text{ odd}$ (20)

for every value of n . Although we have thus reduced the flexibility of our original representation, Eq. (9), as a means of description, we still have undetermined coefficients A_{nm} at our disposal.

If we normalize to the neutral point radius, R , the equations of the F and G contours become ($\bar{\phi} = 0$)

$$F(\rho, \theta) = (\rho \cos \theta) \left(\frac{\cos \theta}{\rho^2} + \sum_{n,m} a_{nm} \rho^n \frac{d P_n^m(\cos \theta)}{d \theta} \right) = 0$$

$$G^{\pm}(\rho, \theta) = \frac{\sin \theta}{\rho^2} + \sum_{n,m} b_{nm} \rho^n P_n^m(\cos \theta) \pm b \rho \sin \theta - K^{\pm} = 0, \quad (21)$$

where

$$\rho = r/R, \quad a_{nm} = A_{nm} R^{n+2}/M, \quad b_{nm} = B_{nm} R^{n+2}/M = -(n+1)a_{nm},$$

$$b = BR^2/M, \quad K^+ = K^+ R^2/M, \quad K^- = 0. \quad (22)$$

The F-contour was derived by requiring it to be tangential to the field line in the noon meridian plane; the G-contour was derived by requiring the magnetic field component tangential to it to satisfy the pressure condition. If we can evaluate the parameters so as to make F and G congruent, then on the resulting contour the boundary conditions Eqs. (1), (4) are satisfied. It should be noted that in the process we would also be specifying the magnetic potentials everywhere, not only in the xz-plane. Using these potentials one can then construct the full free boundary in three dimensions, as we shall demonstrate.

Next we derive the auxiliary conditions which must hold at the neutral point: the G-curve must be continuous, so that

$$\sin \theta_N + \sum_{n,m} b_{nm} P_n^m (\cos \theta_N) - b \sin \theta_N = 0 ; \quad (23)$$

$$\kappa^+ = 2b \sin \theta_N . \quad (24)$$

We can show that the requirements of congruence and that G have continuous first partial derivatives everywhere is equivalent to the hypothesis that N is a neutral point; i.e., $H_N = 0$. The derivatives are already continuous everywhere, with the possible exception of N. Therefore, we require

$$\underline{\nabla} G^- \times \underline{\nabla} G^+ = 0, \text{ for } \theta = \theta_N. \quad (25)$$

Since $G^+ = G^- + 2b\rho \sin \theta + K^*$, we find

$$\partial G^+ / \partial z = \partial G^- / \partial z = \cos \theta_N \partial G^- / \partial \rho - \sin \theta_N \partial G^- / \partial \theta = 0 \quad (26)$$

for $\theta = \theta_N$. This implies that the z-component of the total magnetic field at N vanishes, and that the angle of incidence $\chi = \pi/2$.

The condition, $\partial G / \partial z = 0$, reduces to

$$\sum_{n,m} b_{nm} [n \cos \theta P_n^m(\cos \theta) - \sin \theta \frac{dP_n^m(\cos \theta)}{d\theta}] = 1.5 \sin 2\theta. \quad (27)$$

for $\theta = \theta_N$, $\rho = 1$; which is equivalent to $H_z = 0$ at N.

The congruence of F and G requires $\partial F / \partial z = 0$ at N; this gives rise to the auxiliary condition

$$\sum_{n,m} a_{nm} \left[n \cos \frac{d}{d\theta} - \sin \theta \frac{d^2}{d\theta^2} \right] P_n^m(\cos \theta) = 2 \cos^2 \theta - \sin^2 \theta \quad (28)$$

for $\theta = \theta_N$. We can show that this condition is equivalent to $H_z = 0$ at N.

Since the magnetic field must, by symmetry, have no y-component on the NMC; if $H_z = 0$, then $[H_x \text{ and/or } \partial F / \partial x] = 0$. If $F = \rho \cos \theta \partial W / \partial \theta$, then

$$\frac{\partial F}{\partial z} = \frac{\partial W}{\partial \theta} - \sin \theta \cos \theta \frac{\partial^2 W}{\partial \theta^2} + \rho \cos^2 \theta \frac{\partial^2 W}{\partial \rho \partial \theta}, \quad (29)$$

but

$$H_X = \sin \theta \left(2 \frac{\partial W}{\partial \rho} + \rho \frac{\partial^2 W}{\partial \rho^2} \right) + \cos \theta \frac{\partial^2 W}{\partial \rho \partial \theta} + \frac{\cos \theta}{\rho} \frac{\partial W}{\partial \theta}, \quad (30)$$

and application of Eqs. (16) and the congruence condition, Eq. (19), yields

$$2 \frac{\partial W}{\partial \rho} + \rho \frac{\partial^2 W}{\partial \rho^2} = - \frac{\partial^2 W}{\partial \rho \partial \theta^2} + \frac{\sin \theta}{\rho \cos \theta} \frac{\partial W}{\partial \theta}, \quad (31)$$

so that $\partial F / \partial z = \rho \cos \theta H_X = 0$ at N. Thus, if $\theta_N \neq \pi/2$, then $H_X = 0$; N is neutral.

From Eq. (15) we have

$$\lim_{\theta \rightarrow \theta_N} \partial F / \partial x = - \lim_{\theta \rightarrow \theta_N} (H_Z / H_X) (\partial F / \partial z) = - \cos \theta_N \left(\lim_{\theta \rightarrow \theta_N} H_Z \right) = 0 \quad (32)$$

Therefore, we must add one more auxiliary condition to insure that the F-contour is horizontal at N:

$$\frac{\partial^2 F}{\partial z^2} = \cos^2 \theta \frac{\partial^2 F}{\partial \rho^2} - 2 \sin \theta \cos \theta \frac{\partial^2 F}{\partial \rho \partial \theta} + \sin^2 \theta \frac{\partial^2 F}{\partial \theta^2} = 0 \quad (33)$$

for $\theta = \theta_N$.

Finally, for the sake of convenience, we shall also require that F and G⁻ intersect at $\theta = 0$, $\rho = \rho_0$; by symmetry the gradients of the surfaces are radial at this point. This requirement will give us two additional independent conditions; the first is equivalent to $F(\rho_0, 0) = 0$,

$$1 + \frac{1}{2} \sum_{n=1}^{\mu} a_{n1} n(n+1) \rho_0^{n+2} = 0, \quad (34)$$

since

$$\lim_{\theta \rightarrow 0} \frac{d p_n^m(\cos \theta)}{d \theta} = \begin{cases} + \frac{1}{2} n(n+1), & m = 1 \\ 0, & m \neq 1, \end{cases} \quad (35)$$

which can be derived from the well-known formula (Jahnke, et al., 1960, p. 114)

$$p_n^m(\cos \theta) = \sin^m \theta d^m p_n(\cos \theta) / (d \cos \theta)^m,$$

and the series expansion for $P_n^m(\cos \theta)$.

The requirement that $G^-(\rho_0, 0) = 0$ is identically satisfied; we can also show that $\partial F / \partial \theta = 0$ identically for $\theta = 0$. Since this point satisfies $F = \rho_0 \partial W / \partial \theta = 0$, then

$$\frac{\partial F}{\partial \theta} = \frac{\partial^2 W}{\partial \theta^2}. \quad (36)$$

Furthermore, the congruence condition,

$$\frac{\partial^2 W}{\partial \theta^2} = - \tan \theta \frac{\partial W}{\partial \theta} = 0 \text{ at } \theta = 0, \quad (37)$$

substituted into Eq. (16) (Laplace), yields

$$\frac{\partial^2 W}{\partial \theta^2} = - \frac{\partial}{\partial r} \left(r^2 \frac{\partial W}{\partial r} \right) = 0 \text{ at } \theta = 0, \quad (38)$$

since W depends on terms with factors $P_n^m(1)$ which vanish for $m \geq 1$. Thus, the symmetry of the surface at the apex of the magnetosphere is "built into" our representation by virtue of the congruence condition.

Finally, we have the symmetry condition on G^- :

$$\lim_{\theta \rightarrow 0} \frac{\partial G^-}{\partial \theta} = 1 + \frac{1}{2} \sum_{n=1}^{\infty} b_{n1} n(n+1) \rho_0^{n+2} - b \rho_0^3 = 0, \quad (39)$$

since $\lim_{\theta \rightarrow 0} dP_n^m(\cos \theta)/d\theta = n(n+1)/2$ for $m = 1$, and zero otherwise.

We now wish to make F and G coincide as closely as possible on the assumption that the resulting curves will, at least over some sizable region, be a good approximation to the (assumed) unique solution which lies in both families, F and G , as defined in Eqs. (13) and (18). In Eqs. (21) there are $2 + \mu(\mu+1)/2$ unknowns, b, κ^+, a_{nm} ($\kappa^- = 0, b_{nm} = -(n+1)a_{nm}$); the congruence condition, Eq. (20), yields $(\mu-1)$ independent equations (it is identically satisfied for $n = 1$); there are seven auxiliary equations, (23), (24), (27), (28), (33), (34), and (39), in which two more unknowns, ρ_0 and θ_N , are introduced. Thus we have a system of $(\mu+6)$ equations in $4 + (\mu+1)/2$ unknowns, which we can solve by requiring

the F- and G-contours to intersect at $\mu(\mu-1)/2 - 2$ selected values of θ (we have already required intersection at $\theta = 0$, and $\theta = \theta_X$). Although there is no sure and certain way of solving such systems of transcendental equations, if one begins with a good approximation to the solution there are methods (e.g., Newton-Raphson) which converge to the right answers. To construct such a good approximation one begins with small values of μ for which the equations are soluble, and gradually builds up solutions for larger and larger μ . This method is illustrated in detail in [Blum, 1963b].

In the lowest-order representation, $\mu = 1$, the system appears over-specified. However, as we shall see in the next section, the congruence condition and Eq. (27) are identically satisfied, while Eq. (39) is not independent of the remaining auxiliary equations. Therefore, the system is soluble for $\mu = 1$.

FIRST ORDER CALCULATIONS -- NOON MERIDIAN CONTOUR

Let us consider the first-order expansion for the induced potentials, and apply the method of the preceding section. Then

$$\Omega' = -2A_{11}r \sin\theta \cos\phi; W' = A_{11}r \sin\theta \cos\phi. \quad (40)$$

The congruence condition, Eq. (20), is identically satisfied. In the normalized system the equations

of the confinement and pressure contours are

$$F = \rho \cos \theta (1/\rho^2 + a_{11}\rho) = 0 \quad ;$$

$$G^{\pm} = \sin \theta (1/\rho^2 - 2a_{11}\rho \pm b\rho) - K^{\pm} = 0, K^{\pm}=0. \quad (41)$$

Although we might expect such a meager representation to be greatly overspecified by all the conditions derived in the preceding section, this does not prove to be the case. These conditions are satisfied by the choice of

$$b = 3 \quad , \quad \theta_N = \pi/2, K^{\pm} = 6, a_{11} = -1, R = (3M/\beta)^{1/3} \quad . \quad (42)$$

Note that G^+ and F are circles of radius unity; thus the apex radius, $r_0=R$, implies that the original GMF is approximately tripled at this point, rather than doubled, which is the assumption usually made in treating this problem. Note also that the $\cos \theta$ factor in F , Eq. (41), yields the field line, $\theta = \pi/2$, as part of the F -curve.

The G^+ curve can be represented by

$$1 + 5\rho^2\eta - 6\rho^2 = 0 \quad ; \quad \xi = z/R \quad ; \quad \eta = x/R \quad , \quad (43)$$

so that the height of the magnetosphere approaches an asymptote, $x = 6R/5$ as z goes to $-\infty$. However, the divergence between F and G^+ does not allow us to rely on G^+ as a valid approximation. Therefore, we must employ a different point of view in order to extend our approximation downstream of the neutral point. We shall change the form of the induced potential and use it to calculate a new G^+ curve. We shall then examine the results to determine whether it is cor-

sistent with the confinement condition, $H_s = H$.

We begin by defining the pressure ratio

$$v^2 = \frac{H^2}{\rho^2 \cos^2 \chi} = \frac{H^2}{H_s^2} \quad (44)$$

on the G-surface. If the surface is precisely correct, then the pressure ratio should be identically unity everywhere. If v^2 is close to unity over a significant region (e.g., comparable to R), then we have reason to believe that it may be a valid approximation to the actual surface. Therefore, we extend the contour downstream by assuming that

$$\Omega' = [B e^{kz} J_1(kx) + B' e^{k'z} J_1(k'x)] \cos \theta, \quad (45)$$

where J_1 is a first-order Bessel function (Jahnke, et al., 1960, Chap. IX) and G^+ connects smoothly at the neutral point. The original potential, Ω_0 , is unaltered, to give a better match between upstream and downstream expressions for the magnetic fields at the boundary $z = 0$. The values of the parameters, B, B', k, k' , may be determined from the conditions that the total magnetic field is zero at N, and the pressure ratio is unity. Since the total field consists of the unperturbed dipole plus the induced field, the first condition implies

$$\partial \Omega' / \partial z = - \partial \Omega_0 / \partial z = 0; \quad \partial \Omega' / \partial x = - \partial \Omega_0 / \partial x = 2M/R^3 \quad (46)$$

at $\theta = \pi/2$.

In order to satisfy the first equation of (46) we arbitrarily select kR , $k'R$ to be the first two zeros of J_1 :

$$kR = 3.8317 ; k'R = 7.0156 . \quad (47)$$

In order to determine B, B' we add the relation

$$(\partial^2 \Omega / \partial x \partial z)_N = 0 , \quad (48)$$

which is derived by applying L'Hospital's Rule to the indeterminate ratio $(\partial \Omega / \partial x)_N / (\partial \Omega / \partial z)_N$ and insures that the pressure ratio is unity at the neutral point (where $dz/dx=0$).

The resulting equations are solved by

$$B = \frac{2k'\beta R}{3k(k'-k)J_0(k)} ; B' = \frac{-2k\beta R}{3k'(k'-k)J_0(k')} \quad (49)$$

The consequent F and G surfaces are depicted in Fig. 3 along with values of the pressure ratio at selected points. It can be seen that it is very close to unity until $z/R \leq -2.5$ when it becomes larger than 1.10. This is due to our retention of the original dipole potential in the downstream representation of G; in fact, the pressure ratio should approach infinity as $z \rightarrow -\infty$. However, the magnetic field at $z/R = -3.0$ is only 1% of the field at the apex of the magnetosphere, which is the region of greatest interest.

If we assume elastic reflection from the magnetopause, then the customary assumption of doubling the original field at the apex yields a value of $r_0 = 9.65 R_e$ (Mariner II data,

Neugebauer and Snyder, 1962). This is somewhat smaller than most experimental estimates; explanations have been suggested by means of a postulated ring current. However, the tripling of the field yields

$$r_0 = 11.2 R_e, \quad (50)$$

which is in better agreement with the results of the Explorer XII probe, (Cahill and Amazeen, 1963). This probe measured the radius of the magnetosphere to be $10.5 - 11.5 R_e$ at about 10° from the apex on magnetically quiet days.

Furthermore, our predicted field of 67γ is in agreement with the measured field of 70γ . This is the region where we would expect to find the best agreement, assuming our mathematical model of the interaction to be correct.

On the downstream extension at $\theta=140^\circ$ this approximation predicts

$$r = 22.4 R_e, \quad (51)$$

in good agreement with the measurements of Explorer X, which found the interface to be at about $22.2 R_e$. This apparent agreement must be treated with caution. For one thing, the predicted magnetic field is only 4.5γ , instead of the measured value of 30γ ; furthermore the idealized model does not account for thermal pressure, which is around $1/100$ of the kinetic pressure and would tend to make the dimensions of the actual magnetosphere everywhere smaller than those of the idealized model. This effect would be most pronounced on the downstream side where the field is weak.

Furthermore, there is the question of how well this first-order calculation approximates the solution to the idealized free-boundary problem. The boundary conditions are reasonably consistent over a large region from $z=R$ to $z=-3R$ which leads us to believe that this constitutes a creditable approximation, particularly in respect of the shape of the ^{ideal} magnetosphere, excluding the region around the neutral point. Concerning the size of the magnetosphere, Professor Leverett Davis has noted that if we evaluate the line integral (Ampère's Law)

$$\oint_C \underline{H} \cdot d\underline{s} = 0 \quad (52)$$

over the correct contour C in the xz-plane shown in Fig.4 we find, using Eq. (12),

$$\oint_C \underline{H} \cdot d\underline{s} = - \int_0^{x_N} \theta \, dx + \int_{x_N}^{x_\infty} \beta \, dx = 0 \quad (52)$$

therefore,

$$x_\infty = 2x_N \quad (53)$$

It is clear that Fig. 3 is not in good agreement with Eq. (23), since $x_\infty = 4x_N/3$. Generally the position of the asymptote is rather sensitive to the position of the neutral point. Since our neutral point is on the x-axis, rather than upstream of it, we would expect a large error to show up in the asymptote. It is believed that the exact solution to the idealized free boundary problem will show $2R/3 < x_N < R$.

If one arbitrarily took $x_N = 5R/6$, this would imply θ_N in the range of 56° to 90° . This is in accord with the most recent calculations of Dr. Gilbert Mead of Goddard Space Flight Center (private communication) who finds $x_\infty = 1.70R$, $\theta_N = 71^\circ$ and the apex radius $z_0 = 0.934R$ by means of the fourth iteration of Beard's approximation (Beard, 1960, Beard and Jenkins, 1962).

If Newton's (pressure) condition is used, then our predicted lengths must be multiplied by $(2)^{1/6}$.

Coordinates of selected points on the downstream extension are given in Table I. Computations were performed by using Newton's method to calculate x for each given z ; final increments δx were always less than 0.0001 in the normalized system.

TABLE I

COORDINATES OF DOWNSTREAM EXTENSION, GMF-SCR INTERACTION

Z	X	Z	X $\div (3M/\beta)^{1/3}$
0.000	1.000	-1.000	1.224
-0.100	1.005	-1.200	1.250
-0.200	1.021	-1.400	1.269
-0.300	1.046	-1.600	1.283
-0.400	1.077	-1.800	1.293
-0.500	1.108	-2.000	1.301
-0.600	1.138	-2.500	1.314
-0.800	1.188	-3.000	1.321

THE MAGNETOSPHERE

The next step in our method is the calculation of the magnetopause in three dimensions. This can be done, in principle, by integrating the first-order partial differential equation given by the pressure condition on the boundary:

$$H^2 = \beta^2 \cos^2 \chi = \beta^2 (\partial f / \partial z)^2 / (\nabla f)^2, \quad (54)$$

where $f(\underline{r}) = 0$ is the equation of the magnetopause. In the process of determining the contours F and G in the noon meridian plane we have also determined an approximation to the induced potential, which we have reason to believe valid near the apex and worsening as we go downstream. Bearing in mind the limitations of the approximation, we shall assume that \underline{H} in Eq. (54) is the magnetic field derived by means of the first-order calculation of the preceding section.

In spherical coordinates, normalized to R, the components of $\underline{h} = \underline{H}/\beta$, are:

$$\begin{aligned} h_\rho &= (2/3)(\rho^{-3}-1) \sin \theta \cos \phi \\ h_\theta &= -(1/3)(\rho^{-3}+2) \cos \theta \cos \phi \\ h_\phi &= (1/3)(\rho^{-3}+2) \sin \phi \end{aligned} \quad (55)$$

$$h^2 = h_\rho^2 + h_\theta^2 + h_\phi^2 = (1/9)[(2+\rho^{-3})^2 - 3 \sin^2 \theta \cos^2 \phi (4\rho^{-3} - \rho^{-6})].$$

To the original dipole field we have added the uniform induced field in the x-direction previously derived.

If we express the surface in Cartesian coordinates, Eq. (54) takes on the relatively simple form of the eikonal equation:

$$f(x,y,z)^* = z - Z(x,y) = 0 \quad (56)$$

and since $\nabla f = -\partial Z/\partial x \underline{i} - \partial Z/\partial y \underline{j} + \underline{k}$, then Eq. (54) becomes

$$h^2 = 1/(1 + p^2 + q^2) \quad (57)$$

$$p^2 + q^2 = h^{-2} - 1 \geq 0, \quad (58)$$

where we define

$$p = \partial Z/\partial x ; q = \partial Z/\partial y . \quad (59)$$

Given an equation such as Eq. (59) which can be expressed explicitly by the first-order partial differential equation

$$F(x,y,z,p,q) = 0 ,$$

one may construct a set of simultaneous ordinary differential equations (Courant, 1962, Chap. II)

$$dx/dt = \partial F/\partial p ; dy/dt = \partial F/\partial q ; \quad (60)$$

$$dz/dt = p \partial F/\partial p + q \partial F/\partial q ;$$

$$dp/dt = - (\partial F/\partial x + p \partial F/\partial z) ;$$

$$dq/dt = - (\partial F/\partial y + q \partial F/\partial z) .$$

*Coordinates normalized to R.

These equations yield a family of curves $\{x(t), y(t), z(t)\}$, known as "characteristics," which lie in the desired integral surface, $f(x, y, z) = 0$, determined by the equation $F(x, y, z, p, q) = 0$, plus appropriate boundary conditions. Thus, by constructing this family of curves we have also constructed the surface, f .

There is a well-known theorem (Courant, 1962, pp. 75-84) which states that given some initial curve on the integral surface which is not a characteristic, one can construct the required surface as a unique set of the characteristic strips which pass through the initial curve. In our case we know the initial curve to be the upstream part of the NMC, and also that $q = 0$ and $y = 0$. However, simple substitution shows that this curve is a characteristic, and of itself does not determine a unique integral surface of Eq. (58). However, we may adduce another condition from symmetry: $p = 0$ on the (equatorial) contour which lies in the intersection of the magnetosphere and the plane $\Phi = \pi/2$, since the magnetosphere gradient should have no x-component there. If we substitute the conditions $x = 0$, $p = 0$ into the family of characteristic equations, we find that this curve also is a characteristic and satisfies the equation

$$dz/dy = -(h^{-2} - 1)^{1/2} . \quad (61)$$

Solutions of this equation exist; however, at the initial

point $(x,y,z) = (0,0,1)$ the radical vanishes, so we may not immediately assume the solution unique at that point.

Since all characteristic contours describing the desired surface must lie between the NMC and the equatorial contour, they must all pass through the apex. This type of problem is described by Courant (1962, p. 83) as "A particular limiting case of the initial value problem, the case where the initial curve degenerates into a point All characteristic curves through a fixed point P of x,y,u - [our z] space form an integral surface." Such a surface is known as an integral conoid. It is unique, although it may be a surface of several sheets. The idealized magnetosphere must be such a surface regardless of the representation of h .

To avoid difficulty in applying boundary conditions to the characteristics passing through the apex we shall employ an approximation. We express Eq. (56) in spherical coordinates

$$f(\rho, \theta, \phi) = \rho - P(\theta, \phi) = 0 ; \quad (62)$$

$$h^2 = [\partial(\rho \sin \theta)/\partial \theta]^2 / [\rho^2 + (\partial \rho / \partial \theta)^2 + \csc^2 \theta (\partial \rho / \partial \phi)^2] .$$

The symmetry requirement, $p = 0$ for $x = 0$ and $q = 0$ for $y = 0$, may be expressed by

$$\csc \theta (\partial \rho / \partial \phi) = 0 \text{ for } \phi = 0, \pi/2 . \quad (63)$$

Therefore, we may try to integrate the surface by computing the curves $\rho = \rho(\theta, \phi_0)$ for a set of fixed ϕ_0 , starting at the apex, $\theta = 0$, and ignoring the term $\partial\rho/\partial\phi$ in Eq. (62). When we have generated an integral surface in this way, we can then evaluate $\partial\rho/\partial\phi$ numerically between contours in order to see how much of the surface so calculated is consistent with the approximation. We shall arbitrarily set

$$\csc^2\theta (\partial\rho/\partial\phi)^2 \leq 0.04 (\rho^2 + (\partial\rho/\partial\theta)^2) \quad (64)$$

as the limit of the approximation, so that the right side of the differential equation

$$h = [\partial(\rho \sin \theta)/\partial\theta] / \rho^2 + (\partial\rho/\partial\theta)^2 \quad (65)$$

never differs by more than 2% from the right side of Eq. (62).

If we fix $\phi = \phi_0$ then we have $\partial\rho/\partial\theta \rightarrow d\rho/d\theta$ along the contour which is the intersection of the magnetosphere and the plane of constant ϕ . By integrating Eq. (65) numerically in this way, contour-by-contour, it is possible to generate approximately two-thirds of the upstream part of the magnetosphere before the criterion (64) is violated. This region is bounded by the heavy dashed line in Figs. 5 and 6. From this boundary to the plane $z = 0$ we derive the surface from the characteristic equations starting from the dashed boundary as our initial, noncharacteristic curve.

TABLE 2

CONTOURS OF CONSTANT ϕ A. $\phi = 0.1$ radians

θ (radians)	ρ	$\psi(^{\circ})$
0.1	1.000	0.00
0.2	1.000	0.02
0.3	1.000	0.02
0.4	1.000	0.02
0.5	1.000	0.05
0.6	1.000	0.08
0.7	1.001	0.14
0.8	1.001	0.23
0.9	1.001	0.39
1.0	1.002	0.62
1.1	1.003	1.03
1.2	1.004	1.80
1.3	1.005	3.39
1.4	1.007	7.13
1.5	1.011	17.80
1.6	1.020	39.53

C. $\phi = 0.3$ radians

θ	ρ	$\psi(^{\circ})$
0.1	1.000	0.01
0.2	1.000	0.03
0.3	1.001	0.12
0.4	1.002	0.22
0.5	1.004	0.40
0.6	1.006	0.69
0.7	1.008	1.13
0.8	1.011	1.86
0.9	1.015	2.97
1.0	1.020	4.71
1.1	1.026	7.42
1.2	1.034	11.71
1.3	1.045	18.54
1.4	1.061	29.06
1.5	1.084	43.85
1.6	1.118	61.18

B. $\phi = 0.2$ radians

θ	ρ	$\psi(^{\circ})$
0.1	1.000	0.00
0.2	1.000	0.01
0.3	1.000	0.03
0.4	1.001	0.08
0.5	1.001	0.17
0.6	1.002	0.31
0.7	1.003	0.52
0.8	1.005	0.88
0.9	1.007	1.44
1.0	1.009	2.34
1.1	1.012	3.79
1.2	1.015	6.32
1.3	1.021	10.91
1.4	1.028	19.49
1.5	1.041	34.71
1.6	1.062	55.21

D. $\phi = 0.4$ radians

θ	ρ	$\psi(^{\circ})$
0.1	1.000	0.09
0.2	1.001	0.12
0.3	1.002	0.20
0.4	1.004	0.38
0.5	1.007	0.64
0.6	1.010	1.15
0.7	1.014	1.90
0.8	1.020	3.04
0.9	1.026	4.74
1.0	1.035	7.27
1.1	1.045	11.04
1.2	1.059	16.51
1.3	1.078	24.30
1.4	1.103	34.76
1.5	1.137	47.45
1.6	1.187	60.16

Table 2 (cont.)

E. $\phi = 0.5$ radians

θ	ρ	$\psi(^{\circ})$
0.1	1.000	0.08
0.2	1.001	0.17
0.3	1.003	0.27
0.4	1.006	0.51
0.5	1.010	0.94
0.6	1.016	1.63
0.7	1.022	2.71
0.8	1.030	4.22
0.9	1.040	6.45
1.0	1.053	9.62
1.1	1.069	14.04
1.2	1.089	20.02
1.3	1.116	27.77
1.4	1.151	37.16
1.5	1.199	47.13
1.6	1.266	55.38

G. $\phi = 0.7$ radians

θ	ρ	$\psi(^{\circ})$
0.1	1.000	0.15
0.2	1.003	0.34
0.3	1.007	0.52
0.4	1.012	0.97
0.5	1.019	1.62
0.6	1.029	2.61
0.7	1.041	4.11
0.8	1.055	6.19
0.9	1.074	9.01
1.0	1.096	12.68
1.1	1.124	17.30
1.2	1.159	22.82
1.3	1.204	29.00
1.4	1.262	35.17
1.5	1.337	40.29
1.6	1.439	42.90

F. $\phi = 0.6$ radians

θ	ρ	$\psi(^{\circ})$
0.1	1.000	0.13
0.2	1.002	0.27
0.3	1.005	0.38
0.4	1.009	0.75
0.5	1.015	1.28
0.6	1.022	2.13
0.7	1.031	3.45
0.8	1.042	5.30
0.9	1.056	7.92
1.0	1.074	11.46
1.1	1.095	16.14
1.2	1.123	22.09
1.3	1.158	29.21
1.4	1.205	37.04
1.5	1.267	44.38
1.6	1.350	49.25

H. $\phi = 0.8$ radians

θ	ρ	$\psi(^{\circ})$
0.1	1.001	0.15
0.2	1.004	0.34
0.3	1.008	0.67
0.4	1.015	1.07
0.5	1.025	1.85
0.6	1.036	3.00
0.7	1.051	4.59
0.8	1.069	6.78
0.9	1.092	9.63
1.0	1.119	13.24
1.1	1.154	17.52
1.2	1.197	22.39
1.3	1.251	27.50
1.4	1.319	32.17
1.5	1.409	35.56
1.6	1.527	36.72

Table 2 (cont.)

I. $\phi = 0.9$ radians

θ	ρ	$\psi(^{\circ})$
0.1	1.001	0.21
0.2	1.004	0.38
0.3	1.010	0.77
0.4	1.019	1.18
0.5	1.030	2.03
0.6	1.014	3.40
0.7	1.062	4.84
0.8	1.083	7.02
0.9	1.110	9.75
1.0	1.143	13.08
1.1	1.183	16.90
1.2	1.234	21.03
1.3	1.297	25.08
1.4	1.376	28.50
1.5	1.478	30.63
1.6	1.612	30.88

K. $\phi = 1.1$ radians

θ	ρ	$\psi(^{\circ})$
0.1	1.001	0.35
0.2	1.006	0.56
0.3	1.014	0.79
0.4	1.025	1.31
0.5	1.039	2.03
0.6	1.058	3.12
0.7	1.081	4.56
0.8	1.110	6.34
0.9	1.144	8.51
1.0	1.187	11.01
1.1	1.238	13.66
1.2	1.302	16.27
1.3	1.380	18.57
1.4	1.477	20.21
1.5	1.601	20.85
1.6	1.761	20.34

J. $\phi = 1.0$ radians

θ	ρ	$\psi(^{\circ})$
0.1	1.001	0.26
0.2	1.005	0.49
0.3	1.012	0.78
0.4	1.022	1.35
0.5	1.035	2.11
0.6	1.051	3.21
0.7	1.072	4.84
0.8	1.097	6.86
0.9	1.128	9.36
1.0	1.166	12.31
1.1	1.212	15.59
1.2	1.269	18.94
1.3	1.340	22.04
1.4	1.429	24.44
1.5	1.543	25.69
1.6	1.692	25.43

L. $\phi = 1.2$ radians

θ	ρ	$\psi(^{\circ})$
0.1	1.001	0.22
0.2	1.007	0.41
0.3	1.015	0.70
0.4	1.027	1.13
0.5	1.044	1.82
0.6	1.064	2.76
0.7	1.090	4.00
0.8	1.121	5.49
0.9	1.159	7.24
1.0	1.205	9.21
1.1	1.261	11.25
1.2	1.330	13.21
1.3	1.414	14.83
1.4	1.518	15.90
1.5	1.650	16.17
1.6	1.820	15.60

Table 2 (cont.)

M. $\phi = 1.3$ radians

θ	ρ	$\psi(^{\circ})$
0.1	1.002	0.35
0.2	1.007	0.42
0.3	1.016	0.57
0.4	1.030	0.97
0.5	1.047	1.46
0.6	1.069	2.20
0.7	1.097	3.14
0.8	1.130	4.29
0.9	1.171	5.59
1.0	1.220	7.02
1.1	1.280	8.49
1.2	1.352	9.85
1.3	1.441	10.94
1.4	1.551	11.57
1.5	1.689	11.66
1.6	1.866	11.15

O. $\phi = \pi/2$ radians

θ	ρ	$\psi(^{\circ})$
0.1	1.002	0.00
0.2	1.008	0.00
0.3	1.018	0.00
0.4	1.032	0.00
0.5	1.051	0.00
0.6	1.075	0.00
0.7	1.105	0.00
0.8	1.141	0.00
0.9	1.185	0.00
1.0	1.238	0.00
1.1	1.302	0.00
1.2	1.379	0.00
1.3	1.473	0.00
1.4	1.590	0.00
1.5	1.735	0.00
1.6	1.920	0.00

N. $\phi = 1.4$ radians

θ	ρ	$\psi(^{\circ})$
0.1	1.002	0.26
0.2	1.008	0.36
0.3	1.017	0.51
0.4	1.031	0.66
0.5	1.050	1.05
0.6	1.073	1.44
0.7	1.102	2.08
0.8	1.137	2.81
0.9	1.179	3.66
1.0	1.231	4.57
1.1	1.293	5.47
1.2	1.368	6.30
1.3	1.460	6.94
1.4	1.574	7.27
1.5	1.717	7.28
1.6	1.899	6.93

TABLE 3

CHARACTERISTICS CLASSIFIED BY INITIAL CONDITIONS $(x_0, y_0, z_0, p_0, q_0)$ A. $(0.988, 0.099, 0.171, -5.033, 0.253)$ E. $(0.747, 0.408, 0.609, -1.101, -0.265)$

ρ	$\theta(\text{rad})$	ϕ	$\psi(^{\circ})$	ρ	$\theta(\text{rad})$	ϕ	$\psi(^{\circ})$
1.008	1.420	0.099	8.46	1.048	0.963	0.497	8.20
1.010	1.470	0.098	13.37	1.056	1.024	0.484	10.26
1.012	1.520	0.097	21.81	1.064	1.083	0.472	12.65
1.016	1.570	0.095	33.36	1.072	1.139	0.460	15.42

B. $(0.928, 0.188, 0.368, -2.309, -0.054)$

1.016	1.211	0.199	6.67	1.080	1.193	0.450	18.62
1.019	1.264	0.195	8.54	1.089	1.245	0.439	22.30
1.021	1.315	0.191	11.56	1.098	1.295	0.430	26.49
1.024	1.366	0.188	15.41	1.108	1.344	0.420	31.19
1.028	1.416	0.185	20.71	1.120	1.392	0.411	36.39
1.032	1.466	0.181	27.89	1.132	1.439	0.402	42.02
1.038	1.515	0.178	37.10	1.146	1.484	0.392	47.93
1.047	1.573	0.174	49.79	1.161	1.529	0.383	53.92

F. $(0.683, 0.467, 0.657, -0.930, -0.303)$ C. $(0.848, 0.262, 0.509, -1.542, -0.158)$

1.024	1.062	0.299	6.16	1.059	0.914	0.596	8.23
1.027	1.118	0.292	7.84	1.069	0.978	0.579	10.30
1.031	1.173	0.285	9.93	1.079	1.039	0.564	12.66
1.035	1.227	0.279	12.54	1.089	1.097	0.550	15.34
1.039	1.279	0.273	15.82	1.099	1.152	0.537	18.36
1.044	1.330	0.267	19.97	1.110	1.205	0.525	21.74
1.050	1.380	0.262	25.17	1.121	1.256	0.513	25.49
1.056	1.429	0.257	31.59	1.134	1.306	0.502	29.60
1.063	1.477	0.251	39.27	1.147	1.354	0.491	34.04
1.072	1.525	0.246	48.02	1.161	1.400	0.480	38.75
1.083	1.572	0.240	57.40	1.176	1.446	0.469	43.62

D. $(0.802, 0.339, 0.559, -1.302, -0.215)$

1.036	1.012	0.398	7.56	1.193	1.490	0.458	48.52
1.042	1.071	0.388	9.50	1.211	1.532	0.447	53.28
1.048	1.127	0.379	11.83	1.230	1.573	0.436	57.69
1.053	1.182	0.370	14.61				
1.060	1.235	0.362	17.94				
1.066	1.286	0.354	21.90				
1.074	1.337	0.346	26.59				
1.082	1.386	0.339	32.06				
1.091	1.434	0.331	38.30				
1.102	1.481	0.324	45.23				
1.114	1.527	0.316	52.64				
1.128	1.571	0.308	60.22				

G. $(0.612, 0.515, 0.702, -0.780, -0.332)$

1.064	0.850	0.700	7.42				
1.077	0.920	0.678	9.38				
1.089	0.985	0.660	11.60				
1.101	1.045	0.643	14.10				
1.114	1.103	0.627	16.87				
1.127	1.157	0.613	19.92				
1.140	1.210	0.599	23.26				
1.154	1.260	0.586	26.75				
1.169	1.310	0.574	30.68				
1.185	1.356	0.562	34.70				
1.202	1.402	0.549	38.82				
1.220	1.446	0.538	42.96				
1.240	1.488	0.525	47.02				
1.260	1.529	0.514	50.85				
1.283	1.570	0.502	52.34				

H. (0.535, 0.550, 0.745, -0.648, -0.351) J. (0.478, 0.744, 0.701, -0.566, -0.460)

ρ	θ	ϕ	$\psi(^{\circ})$	ρ	θ	ϕ	$\psi(^{\circ})$
1.070	0.800	0.800	6.70	1.128	0.900	1.000	9.42
1.085	0.875	0.774	8.56	1.152	0.970	0.976	11.41
1.099	0.943	0.752	10.67	1.176	1.034	0.955	13.57
1.114	1.007	0.733	13.03	1.200	1.094	0.936	15.87
1.128	1.066	0.715	15.62	1.225	1.149	0.919	18.28
1.143	1.123	0.699	18.44	1.251	1.202	0.903	20.74
1.159	1.176	0.684	21.48	1.277	1.251	0.888	23.25
1.175	1.228	0.669	24.72	1.304	1.298	0.874	25.74
1.192	1.277	0.655	28.11	1.333	1.343	0.860	28.20
1.211	1.324	0.642	31.55	1.362	1.385	0.847	30.59
1.230	1.370	0.629	35.22	1.393	1.427	0.834	32.88
1.250	1.414	0.616	38.80	1.424	1.464	0.822	35.04
1.271	1.456	0.604	42.31	1.457	1.501	0.809	37.07
1.294	1.497	0.591	45.65	1.491	1.536	0.797	38.91
1.328	1.536	0.579	48.74	1.527	1.570	0.786	40.59
1.343	1.574	0.566	51.50				

I. (0.512, 0.645, 1.096, -0.616, -0.405)

ρ	θ	ϕ	$\psi(^{\circ})$	ρ	θ	ϕ	$\psi(^{\circ})$
1.104	0.880	0.889	9.06	1.182	0.991	1.087	10.93
1.123	0.950	0.865	11.16	1.211	1.055	1.067	12.81
1.142	1.014	0.844	13.48	1.240	1.113	1.050	14.79
1.162	1.074	0.826	15.98	1.270	1.168	1.034	16.82
1.181	1.130	0.808	18.65	1.301	1.219	1.019	18.87
1.201	1.184	0.792	21.45	1.332	1.268	1.005	20.92
1.222	1.234	0.777	24.35	1.365	1.313	0.992	22.92
1.244	1.283	0.762	27.32	1.400	1.356	0.979	24.86
1.267	1.329	0.748	30.31	1.433	1.397	0.967	26.73
1.291	1.373	0.735	33.27	1.469	1.436	0.956	28.49
1.316	1.415	0.722	36.17	1.506	1.473	0.944	30.15
1.343	1.456	0.709	38.94	1.544	1.508	0.934	31.69
1.370	1.495	0.696	41.55	1.584	1.547	0.921	33.11
1.399	1.543	0.683	43.95	1.624	1.572	0.913	34.38
1.429	1.568	0.671	46.11				

L. (0.368, 0.945, 0.651, -0.421, -0.573)

ρ	θ	ϕ	$\psi(^{\circ})$
1.206	1.000	1.200	9.49
1.238	1.064	1.182	10.97
1.272	1.122	1.167	12.52
1.306	1.177	1.153	14.11
1.342	1.228	1.140	15.70
1.378	1.275	1.139	17.28
1.415	1.320	1.117	18.81
1.453	1.362	1.106	20.28
1.493	1.402	1.096	21.68
1.533	1.439	1.086	22.95
1.575	1.475	1.077	24.24
1.617	1.508	1.068	25.39
1.661	1.540	1.059	26.45
1.706	1.570	1.051	27.43

Tables 2 and 3 give coordinates of selected points on constant- ψ and characteristic contours, respectively.

Let us define an angle ψ such that

$$\tan \psi = \frac{|\underline{h} \cdot \underline{\nabla} f|}{|\underline{h} \times \underline{\nabla} f|} ; \quad (66)$$

\underline{h} is known, and the gradient of f is calculated numerically from $(\rho, \theta, \partial \rho / \partial \theta, \partial \rho / \partial \Phi)$ or (p, q) at the point in question, depending upon which representation is more convenient. The value of ψ is also listed in Tables 2 and 3. The light dashed line in Figs. 5 and 6 is the boundary of the region of the magnetopause over which $\psi \leq 10^\circ$. The line composed of alternating dots and dashes marks the boundary for $\psi \leq 25^\circ$.

As expected, we find that agreement with the confinement condition ($\psi = 0$) worsens as we move away from the magnetosphere apex. However, the values of ψ are sufficiently small over a significantly large region of the magnetosphere, that we assume our approximation to be valid. Even in the case that $\psi = 25^\circ$, the total field exceeds the tangential field by only 10%. The induced field used here is probably larger than the actual field; it is expected that the surface derived here is an upper limit to the actual solution of the idealized problem.

In this approximation, the magnetosphere may be represented by the empirical formula

$$\rho(\theta, \Phi) = \frac{\alpha(\Phi) \cdot \theta [1 - \delta(\Phi) \cdot \theta^2]}{\sin [\alpha(\Phi) \cdot \theta]} , \quad (67)$$

$$\alpha(\Phi) = (8/5) \sin (7\Phi/5) ,$$

$$\delta(\Phi) = (\Phi/4) \sin (15\Phi/8) ,$$

$(0 \leq \theta \leq \pi/2 , 0 \leq \Phi \leq \pi/2)$

to within 4%.

A convenient representation for the intersection of the magnetosphere and the xy-plane is given by

$$y^2 = 0.2263 \rho^{5/3} (\rho^3 - 1) , \quad (68)$$

where $\rho^2 = x^2 + y^2$. Comparison with the $z = 0.00$ contour of Fig. 2 shows that Eq. (68) is accurate to within 0.2%.

These calculations may be performed for higher-order congruence approximations without any fundamental change in the method illustrated here. Additional refinement would allow us to begin the extension further downstream; by adding terms to the extension formula, Eq. (45), we should be able to match the upstream and downstream fields more closely. This would give an improved approximation to the fields inside the magnetosphere, and allow us to extend the three-dimensional surface further downstream. Ultimately, one could use the surface so obtained as the first trial in a three-dimensional relaxation calculation (Cartesian coordinates). If the accuracy of the co-location and extension is sufficient, this last step could be omitted.

Bibliography

Beard, D.B., The interaction of the terrestrial magnetic field with the solar corpuscular radiation. J. Geophys. Res., 65, 3559-3568, 1960.

Beard, D.B., Interaction of the terrestrial magnetic field with the solar corpuscular radiation. J. Geophys. Res., 67, 477-483, 1962_a.

Beard, D.B., and Jenkins, E.B., The magnetic effects of magnetospheric surface currents. J. Geophys. Res., 67, 3361-3367, 1962_b.

Blum, R., The interaction between the geomagnetic field and the solar corpuscular radiation. Icarus 1, 459-488, 1963_a.

Blum, R., The interaction of the geomagnetic field and the solar corpuscular radiation. Stanford University, Microwave Laboratory Report No. 1035, May, 1963_b.

Cahill, L.J., and Amazeen, P.G., The boundary of the geomagnetic field. J. Geophys. Res. 7, 1835-1843, 1963.

Courant, R., Methods of Mathematical Physics, Vol. II. Interscience, New York, 1962.

Dungey, J.W., Cosmic Electrodynamics. Cambridge University Press 1958.

Heppner, J.P., Ness, N.F., Searce, C.S. and Skillman, T.L., Explorer 10 Magnetic Field Measurements. J. Geophys. Res. 68, 1-46, 1963.

Hurley, J., Interaction of a streaming plasma with the magnetic field of a line current. Phys. Fluids 4, 109-111, 1961_a.

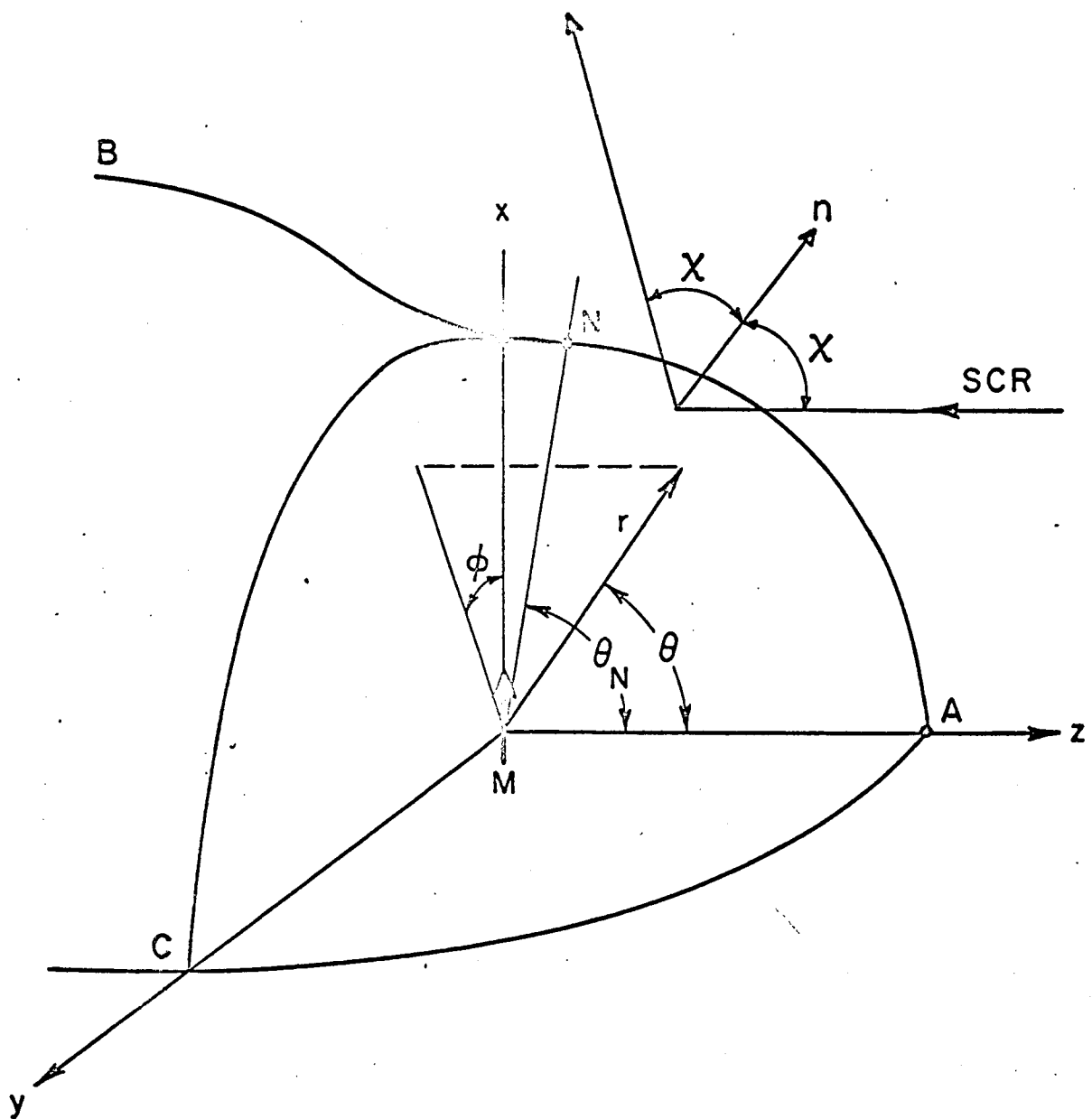
Hurley, J., Interaction of a streaming plasma with the magnetic field of a two-dimensional dipole. Phys. Fluids 4, 854-859, 1961_b.

Janke, E., Emde, F., and Lösch, F., Tables of Higher Functions 6th ed., McGraw-Hill, New York, 1960.

Neugebauer, M., and Snyder, C.W., The mission of Mariner II: preliminary observations, solar plasma experiment. Science 138, 1095-1097, 1962.

List of Figures

1. GMF-SCR interaction, schematic.
2. Boundary conditions in the noon meridian plane.
3. GMF-SCR interaction, first-order approximation; $R^3 = (3M/\beta)$.
4. Contour of integration, $\epsilon \rightarrow 0$.
5. Projection of magnetopause on the xy-plane.
6. Perspective of magnetosphere.



MAGNETOSPHERE
BOUNDARY

REFLECTED
PARTICLES

FIELD LINE

INCIDENT PARTICLES

